Open Access Journal

Journal of Sustainable Research in Engineering Vol. 4 (1) 2017, 1-11

Journal homepage: http://sri.jkuat.ac.ke/ojs/index.php/sri

Analysis of Temperature Distribution in Laser Assisted Metal Polymer (LAMP) Joining

Francis Njihia[1*], Bernard W. Ikua[1], Alphonse Niyibizi[2]

[1]*Department of Mechatronic Engineering, JKUAT, P.O Box 62000-0020, Nairobi, Kenya*

[2]*Department of Physics, DeKUT, P.O Box 657-10100, Nyeri, Kenya*

[*]*Corresponding Author - E-mail: francnjihia2003@gmail.com*

Abstract: The need for lightweight components, reduced cost, and improved efficiency in modern manufacturing has led to increasing interest towards hybrid polymer-metal components with optimized characteristics. This has resulted to development of new components with tailored properties for application in aerospace, energy generation, medical and electronics as well as for consumer goods. Laser Assisted Metal to Polymer (LAMP) joining is a modern technique used in joining metals to polymers by irradiation of a laser beam to the metal-polymer interface to melt the polymer for bonding. During the LAMP process, excessive heat could lead to degradation of the polymer while insufficient heat could lead to uneven melting. These results to improper joints, and therefore, there is a need to regulate the amount of heating in the process. Delivery of the thermal energy by the laser beam is affected by parameters such as laser beam power, scanning speed, the absorptivity of the materials, and the contact pressure at the interface. To attain uniform temperature distribution and optimum temperature values for proper melting of the polymer, a careful selection of these parameters is essential. In this paper, a finite element model is developed to investigate the influence of different laser parameters on temperature distribution at the interface during LAMP joining. This model is used to predict the depth and width of the molten zone, and temperature distribution within the heat-affected zone. Simulation runs are carried out for the joining of Polyethylene Terephthalate (PET) polymer and stainless steel plate (SUS304) materials. Their common application in LAMP joining provides the motivation to use them as case study for this research. From the analysis, it is seen that increasing laser power and decreasing laser scan speed leads to the increase of the interface temperatures and dimensions of the molten zone. A comparison is made for the predicted width of melt with experimental bond width. The results for the range of parameters used are in good agreement and have a maximum deviation of 6%.

Keywords polymer-metal joints, LAMP joining, thermal simulation

1. Introduction

The requirement for energy saving, lightweight and cost-effectiveness in manufacturing industries has led to development of new strategies and novel processes for products with enhanced properties. This has led to the use of polymers and polymer-based composite as alternative materials in different application. However, polymers cannot fully substitute metals in some industrial applications, especially in situations where structural strength is required.

Metals possess high strength, toughness, high thermal and electrical conductivity, and high heat resistance, while polymers have advantages of low weight, high impact and corrosion resistance, and excellent deformability properties. Material hybridization offers a compromise and complementarity solution between all metal and all-polymer structures. Laser assisted metal to

polymer (LAMP) joining is a process for joining polymers and metals together using laser technology [1]. It involves the propagation of the laser beam at the metal-polymer interface to melt the polymer for bonding with the metal surface. The process offers higher production flexibility, non-stringent requirements on surface preparation, and low possibility of contamination during the joining process as compared to the conventional techniques [2].

Kawahito et al. [3] first introduced the laser joining approach of metal to polymers. Katayama et al. [4] later studied the mechanism of laser joining of polymers and metals. In these pioneering works, joints of stainless steel with polyethylene terephthalate (PET), polyamide (PA), polycarbonate (PC) and polypropylene (PP) were formed and tested for strength. They obtained high shear strength of the joints. Further investigations were conducted to study the mechanisms of LAMP joining using different materials [5],[6]. It was reported, that it is not only the mechanical bonding that causes the joint formation but also physical and chemical bonding mechanisms. The introduction of LAMP was initially motivated by the need for lightweight, energy-saving and cost-effective components in aerospace and automobile industries. However, the research of laser polymer-metal joining was later initiated for other applications such as the medical equipment and electronic industries. Georgiev et al. [7] developed a laser bonding process for the production of micro electro mechanical systems (MEMS). Both Kapton® FN PI film and Teflon® fluorinated propylene film were bonded with Titanium film. Wang et al. [8] demonstrated the laser joining technique using polyethylene terephthalate (PET) film bonded to Ti foil for the packaging of bio-implantable devices such as pacemakers.

Different studies have reported on various approaches to undertake the laser joining technique. Holtkamp et al. [9] developed a new joining method named “Laser-Induced Fusion Techhnology”(LIFTEC). This technology is based on the fact that most thermoplastics are transparent, or at least translucent to common laser wavelength, in the unpigmented state. A metal or ceramic component heated by laser radiation through the polymer is pressed onto the polymer after achieving sufficient plasticity. Roesner et al. [10] introduced a new approach of using laser radiation for ablating the metal surface to create microstructures with undercut grooves before joining. The molten polymer expands into the structures during the joining process.

In the past few years, several studies[11]–[15] have been conducted to evaluate the feasibility of joining different polymer metal combinations. In addition, there are studies directed towards improving the joint characteristics. Cenigaonaindia et al. [16] proposed a new approach to perform the laser transmission joining (LTJ). The proposed technology was intended to improve the strength of hybrid structures by increasing the amount of molten polymer trapped in the metal surface cavities. Roesner et al. [17] reported that laser micro-structuring of the metal surface increases the bond strength with the polymer. Recently, several studies [18]–[21] have been conducted toward improving the stability of LAMP joined parts.

Studies on modeling and simulation of LAMP joining have also gained interest in the past few years in an attempt to predict different outcomes and optimize various multiple parameters during the joining process. Shashi et al. [22] conducted an optimization of laser transmission joining parameters on bond strength of PET and 316 L stainless steel sheets joint using response surface methodology (RSM). They developed a mathematical model between laser transmission joining parameters and desired response (joint strength). Using analysis of variance (ANOVA), the relation between the parameters and strength was presented. The statistical approach however failed to relate the effect of parameters in consideration, to any mechanism occurring during the joining process. Tillman et al. [23] conducted an experimental optimization in laser welding of metal to polymer of stainless steel plate type SUS304 and Polyethylene Terephthalate (PET) polymer sheet. The study considered the optimization of two influential process parameters, that is, the laser power, and welding speed. Microstructure features, tests of tensile shear strength, investigation of the fracture location, and morphology were used to evaluate the joint performance. The experimentation work however failed to fully explain the actual effects of parameters in the process resulting to the changing values of fracture load. Particularly, the relationship of parameters with temperature distribution at the interface responsible for melting the polymer was not clear in the work. Acherjee et al. [24] conducted a finite element simulation of diode laser transmission welding of dissimilar materials. They simulated the temperature field in the laser transmission welding process for joining Polyvinylidene fluoride (PVDF) to titanium using a distributed moving heat flux. Different temperature values were predicted for Titanium and PVDF. In this work, no investigation on the effects of process parameters on the developed temperature field joint was conducted, and therefore

variations were unaccounted for. Rodríguez et al. [25] combined experimental and numerical approaches to study the influence of the structuring geometry on the behavior of the adhesion force between dual phase steel (DP1000) and glass reinforced polyamide (PA6-GF30). A clear impact of metal structuring on the breaking force was demonstrated from the experiment. In this study, effects of laser beam parameters on the joining process were not considered.

In the previous works of optimization, a lot of effort has been focused on experimental studies, where strength, microstructure evolution, morphology and distortion of the joined assembly are the only basis of optimization. The experimental approach is not only expensive but also time-consuming. Little work has focused on process simulation, where the acting physical phenomena and the resulting local temperature field is studied. The influence of different laser input parameters on the joining process has also not fully been explored. The simulation of the process helps to convey information relating to process conditions for improved accuracy, predictability, and consistency in a cost effective way.

The main aim of this study is to develop a finite element model for predicting the temperature profile and bond width during LAMP process. A numerical analysis for temperature distribution at the polymer-metal interface, and optimization of the laser beam and process parameters is conducted. Focus is on the laser beam power and scanning speed. The model will be capable of predicting thermal cycles, dimensions of the molten zones and areas with lack of melting or overheating.

2. Simulation Setup

2.1 Mathematical Formulation

The heat equation is used as a differential statement of thermal energy balance in the materials. The content of thermal energy in a material changes, if energy is added to its bounding surface, generated, or absorbed within the body. The temperature variation can be expressed as;

$$\frac{\partial T}{\partial t} = \nabla . \alpha \nabla T + \frac{g(x,t)}{\rho\, C_p} \qquad (1)$$

where T is the temperature, α is the thermal diffusivity, ρ is the material density, $g(x,t)$ is the heat generation term and C_p is the specific heat capacity of the material.

The laser beam movement relative to the workpiece requires the contribution of a translational motion sub-node u that defines the velocity. The contribution describes the effect of a moving coordinate system, which is required to model the moving heat source. When parts of the model are moving in the material frame, the energy balance equation becomes;

$$\rho C_p \left[\frac{\partial T}{\partial t} + u.\nabla T\right] = k\nabla^2 T + g(x,t) \qquad (2)$$

The right-hand side of this heat equation includes the contribution of heat source, which describes the heat generation within the domains. It models a moving laser beam with a Gaussian distribution, due to the intensity profile of a propagated laser beam. The volumetric heating, as well as the boundary conditions balance the temperature inside the material. Heat exchange due to radiation and convection at the surfaces are accounted for in the boundary conditions.

The Newton's law of cooling for convection heat transfer is expressed as:

$$\dot{q}_c = Ah(T_s - T_\infty) \qquad (3)$$

where h is the convection heat transfer coefficient, T_s is surface temperature, and T_∞ is the temperature of surrounding surfaces. All the surfaces of the work piece except the top metal surface and bottom polymer surface are assumed to transfer heat by natural convection to the environment since they are exposed to the surroundings.

Thermal radiation from the metal surface is also considered. The rate of radiation heat transfer can be expressed as:

$$\dot{q}_r = A\sigma\epsilon(T_s^4 - T_\infty^4) \qquad (4)$$

where σ is the Stefan Boltzmann constant and ε is the emissivity of the metal.

The mode of heat distribution for a laser radiation can be defined in Gaussian form. The mathematical equation of a Gaussian heat-flux distribution can be expressed as;

$$I(x,y) = \frac{2P}{\pi r_0^2} exp\left(\frac{-2[(x-x_0)^2 + (y-y_0)^2]}{r_0^2}\right) \qquad (5)$$

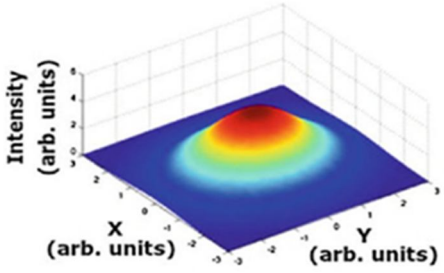

Fig. 1. Gaussian distribution

In which I is the intensity of the laser, P is the laser beam power, r_0 is the radius of the beam, and (x_0,y_0) the coordinates of the laser beam center. The maximum heat intensity is localized at the center of the beam, and by moving away from the center, the intensity decreases exponentially.

2.2 Polymer Heating

The heating of behavior of PET is similar to most thermoplastics. It consists of two stages of transition, including the glass transition and melting. On heat input, the material has a softening point, when the thermal kinetic energy causes the internal rotation within the bonds and sliding of individual molecules. This occurs at glass transition temperature. At a higher temperature, the crystalline regions of the polymer break and the material becomes viscous liquid. This is at the melting temperature. The melting occurs over a range of temperature, depending on degree of crystallization [26]. At melting temperature, the polymer remains as a melt or liquid whose viscosity depends on molecular weight or temperatures on observation[27].

Heat transfer within the polymer is modeled with consideration of phase change to analyze the transition from solid to liquid phase during melting. Modeling the heat transfer with phase change involves solving the heat equation according to the heat capacity formulation after specification of the material properties undergoing the phase change. The apparent heat capacityC_p, used in the heat equation is given by;

$$C_p = \frac{1}{\rho}\left(\theta_1\rho_{ph1}C_{p,\,ph1} + \theta_2\rho_{ph2}C_{p,\,ph2}\right) + C_L \qquad (2)$$

The material phase is modeled by a smooth function, θ, representing the fraction of phase during the transition, and the indices ph1 and ph2 indicate a material in phase 1 or phase 2, respectively. C_L is the distribution of latent heat.

2.3 Materials and Simulation Process

The materials considered in this polymer-metal joining study are Polyethylene Terephthalate (PET) polymer overlapped on stainless steel plate type SUS304. PET is a typical engineering polymer with high laser transparency especially for radiation sources emitting near infrared wavelengths [28]. Its excellent wear resistance, high flexural modulus, superior dimensional stability, and low coefficient of friction make it a multipurpose material for designing mechanical and electromechanical parts. Stainless steel Type 304 is the most versatile and widely used of all types of stainless steel. Its superior mechanical properties and corrosion resistance provide the best all round performance in most industrial applications. The PET-SUS304 material joining has previously been used to study the physical and chemical joining mechanisms associated with the LAMP joining process. Their bonds have produced strong joints [5]. Therefore, they provide an informed basis of study in this thermal simulation analysis.

The material properties required for the heat flow analysis are mainly the thermal conductivity, specific heat and density. The values of these properties for PET and SUS304 are given in Table 1. A finite element model is established based on COMSOL 5.1v modeling software. The model mainly include; heat transfer in solids for heating of the bottom metal domain; heat transfer with phase change for the top PET domain; and heat flux on the top metal boundary to account for the laser heating.

The solutions are uniquely defined, provided that the appropriate initial and boundary conditions are given. The assumptions on which the model is based are: The laser beam has an ideal Gaussian intensity profile; the divergence angle of the beam is small; the incident laser beam is directional and collimated; the surface of both materials are smooth and flat, and effects of fluid gap or surface roughness on heat transfer between the polymer and the metal at the interface are negligible. In addition, the effect of moving molten front in heating of the polymer was considered negligible since the polymer does not melt fully to liquid phase, as is the case with metals.

Table1. Material properties[29], [30]

Properties	**PET**	**SUS304**
Density, (Kg.m-3)	1455	8030
Specific heat capacity, ($J.Kg^{-1}.K^{-1}$)	1200	500
Thermal conductivity, ($W.m^{-1}.K^{-1}$)	0.2	16.2
Coefficient of thermal expansion, (K^{-1})	59.4×10^{-6}	17.3×10^{-6}
Melting temperature range, (K)	475-530	1399
Boiling point, (K)	-	1510
Decomposition temperature, (K)	573	-
Degradation temperature, (K)	600	-
Poisson's ratio	0.4	0.3
Young's modulus, (MPa)	1700	18500

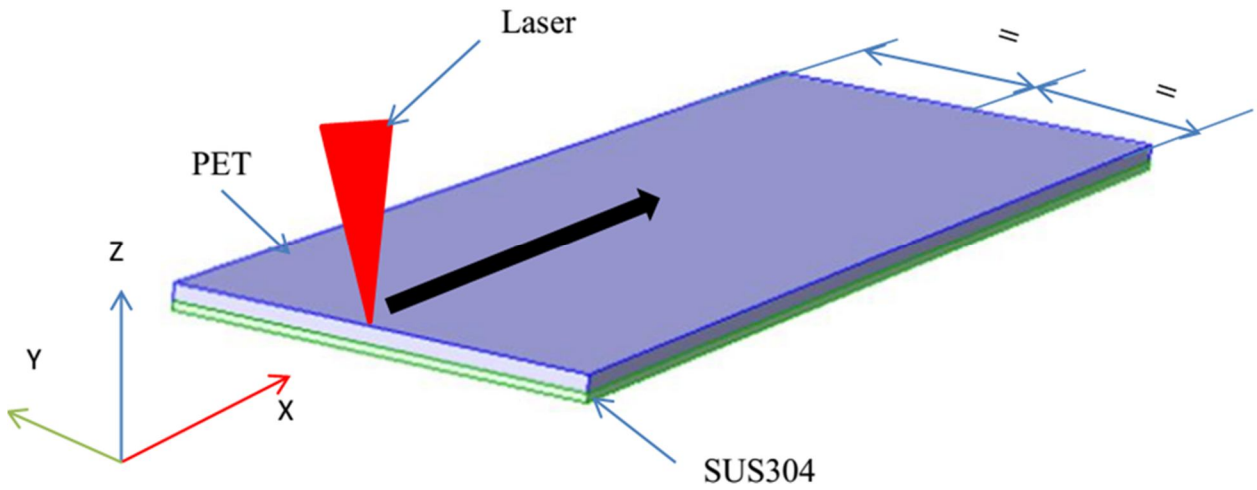

Fig. 2. Component Domains

2.3 Design and Meshing

The model consists of two layers as shown in Figure 2. The top layer represents the polymer (PET) and the bottom one, the metal (SUS304). The width of both materials is 25 mm while the length is 70 mm. The thickness of metal plate is 0.5 mm and that of the polymer is 1mm. The choice of these thicknesses is based on the commonly used material thicknesses for most polymer metal joints. The other dimensions are arbitrarily taken, as they have no effect on the output. The irradiating laser beam will move across the length at the symmetrical point of the width. Therefore, the component width is symmetrized along the laser path in order to have a better view of the thermal process across its depth and width.

The component is fully discretized with a mapped meshing that generates a structured mesh with quadrilateral elements as shown in Figure 3. For mesh convergence test, the sizes of the mesh were altered from a free mesh to refined mesh while finding the solution. The size of the mesh affects accuracy of the results. In this case, the finest mesh available within the COMSOL software was used. The computational time was of little consideration since it was good with the finest mesh.

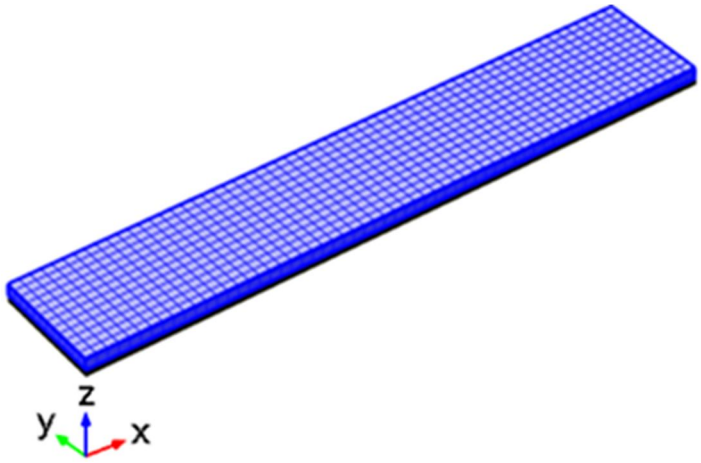

Fig. 3. Component Meshing

3. Results and Discussion

3.1 Joint Interface Temperatures

Figure 4 shows the simulation results on temperature distribution for the laser joining process of PET and SUS304 plate. Simulations are carried out at room temperature of 293K indicated by ▼. The maximum temperatures predicted for various levels of laser power are indicated by ▲. From the figure, it can be seen that the interface temperatures increase with increase in the laser power. The temperatures predicted for the different

laser power are related to thermal properties of PET. For the laser power of 40 W (Fig. 4(a)), the maximum temperature predicted at the interface is 481 K. This temperature is close to the lower limit for melting the polymer (475 K). Being close to the lower melting point, this temperature may be too low to sufficiently melt the polymer, owing to the low conductivity of the polymer. Consequently, a weak bond is likely to be produced. For the laser power of 60 W (Fig. 4(b)), the predicted maximum temperature is 550 K. This is well above the melting point of the polymer, and therefore the polymer is expected to melt sufficiently. Moreover, this temperature is below the decomposition and degradation temperatures of the polymer, and therefore, it guarantees a bond with minimal defects. For the laser power of 70 W (Fig. 4(c)), the maximum predicted temperature is 585 K. This is above the threshold temperature for decomposition (573 K), and therefore the polymer is likely to decompose [23]. Decomposition of the polymer not only leads to high bubble formation, but also alters the chemical structure of the polymer. These conditions are undesirable for proper bonding.

The maximum temperatures predicted for the laser power of 80 W (Fig 4. (d)) is 618 K. This temperature is expected to cause degradation of the polymer [31]. Degradation of polymers causes undesirable change in physical and mechanical properties of the polymer [32]. Figure 5 shows the simulation results on temperature distribution for different laser scan speed in the laser joining process of PET and SUS304. For the laser scan speed of 5 mm/min (Fig. 5(a)), a maximum temperature of 625 K is predicted. At this speed, the resulting temperature is very high and the polymer will degrade and lose its desirable physical and mechanical properties. Maximum interface temperatures of 559 K and 536 K are predicted for the scan speeds of 20 mm/min and 35 mm/min, respectively (Fig. 5(b), (c)). These temperatures are above the upper limit of melting point of the polymer (530 K) and below the decomposition temperatures (573 K). It is expected that at these scan speeds, the polymer will melt sufficiently with minimal defects, thus resulting in proper bonding with the metal surface. The high scan speed of 50 mm/min (Fig. 5(d)) results in relatively lower temperatures, which are insufficient to melt the polymer fully. Hence, this is likely to result in a weak bond.

Thus, it is clearly seen from the analysis that slow scan speeds result in an increase of the delivered energy across the interface, while high scan speeds result in a decrease. This can be attributed to the differences in the residence time of the laser beam, which results in varied heat input and absorption into the material.

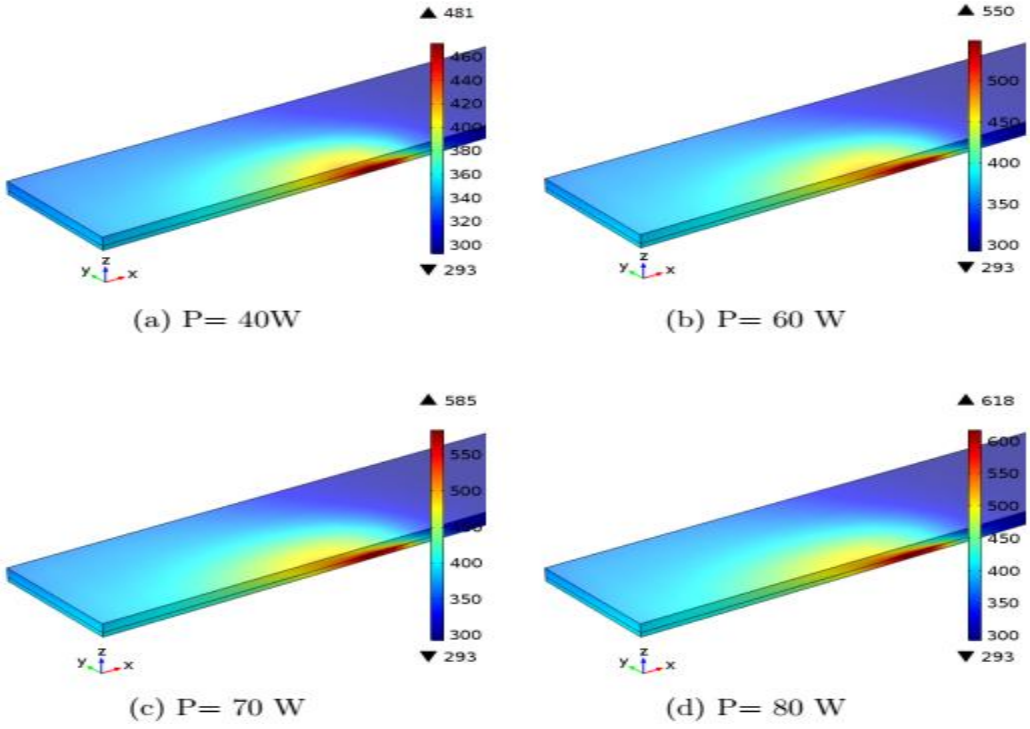

Fig. 4. Interface temperatures for different laser power (Scan speed, 30 mm/min)

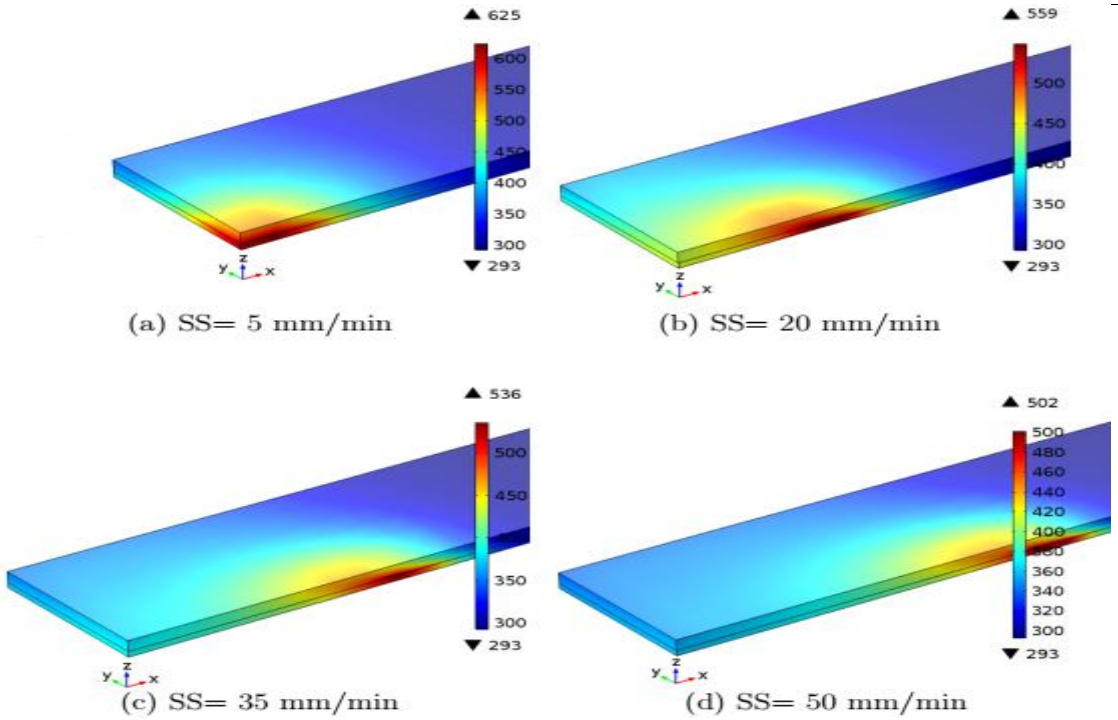

Fig. 5. Interface temperatures for different scan speeds (Laser power, 60 W)

3.2 Temperature Distribution across the Thickness

Figure 6 shows the temperature distribution across the materials thickness for laser power of 60 W and 70 W. The irradiation is from the top side of the polymer as was shown in Fig. 2. The bottom part of the metal plate is the datum and the interface is at 0.5 mm from the datum, which corresponds to the metal thickness. The rest (0.5-1.5 mm) corresponds to the polymer thickness. It can be seen in the figure that the maximum temperatures occur at the interface. It can also be seen that the temperature difference for the metal part is small as compared to that for the polymer. The occurrence of the maximum temperature at the interface can be attributed to the high absorptivity of the laser beam by the metal. The relatively lower difference in temperatures across the metal thickness is due to the metal's high conductivity as compared to that of the polymer.

The depth of melt for the polymer can predicted by temperature distribution from the interface. It can be seen that the minimum melting temperature (475 K) of the polymer occurs at 1 mm and 1.2 mm for laser power of 60W and 70 W respectively. The depths of melt are then determined as 1 - 0.5 = 0.5 mm for the 60 W, and 1.2 - 0.5= 0.7 mm for the 70 W laser.

The predicted depths of melt of the polymer for other laser powers and conditions are deduced in a similar manner. Figure 7 shows the influence of laser power on the depth of melt of the polymer. It can be seen in the figure that as the laser power increases the depth of melt increases. Higher laser power leads to higher absorption of the heat by the metal, which in turn results in increased temperatures, and consequently, larger area of melting.

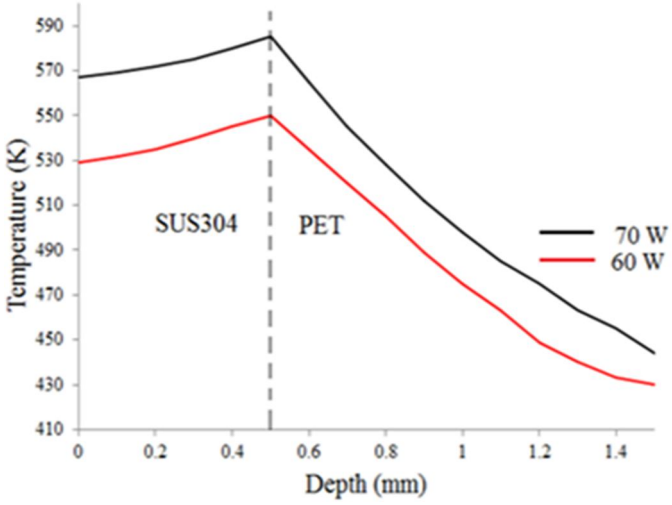

Fig. 6. Temperature distribution for different laser power

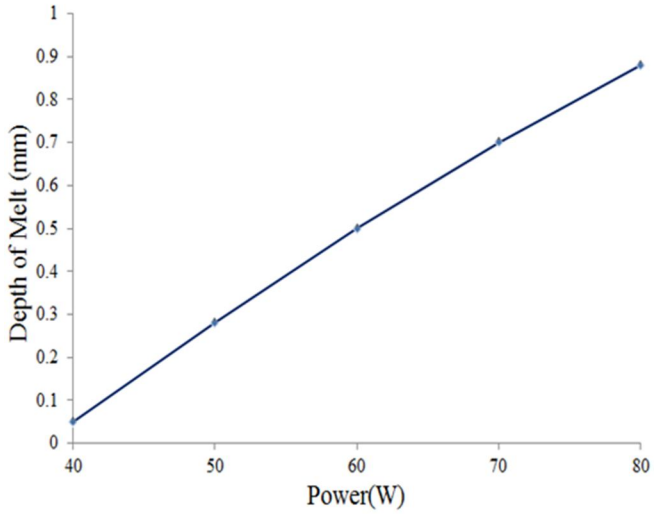

Fig. 7. Influence of laser power on depth of melt (Scan speed, 30 mm/min)

Figure 8 shows the temperature distribution across the depth for scan speeds of 20 mm/min and 35 mm/min. It can be seen in this figure that, the temperatures across the depth for both scan speeds follow the same pattern as discussed earlier, and that the temperatures achieved at scan speed of 20 mm/min are higher than those at scan speed of 35 mm/min. At the minimum melting temperature of the polymer, i.e., 475 K, it can be deduced that the depth of melt is 0.5 mm for the scan speed of 20 mm/min, and 0.3 mm for scan speed of 35 mm/min.

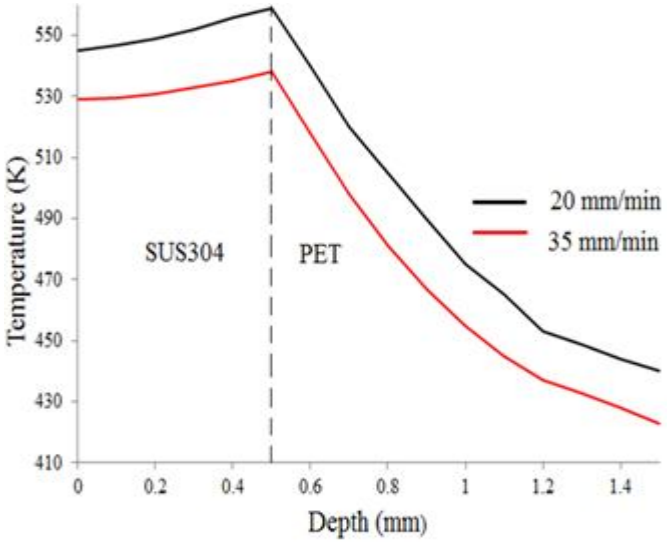

Fig. 8. Temperature distribution across the thickness for different scan speeds.

The influence of laser scan speed on depth of melt is shown in Figure 9. It is seen that depth of melt decreases with increase of scan speed. The depth of melt is 0.85 mm for scan speed of 5 mm/min and about 0.1 mm for scan speed of 65mm/min. Thus hardly any melting occurs above this speed.

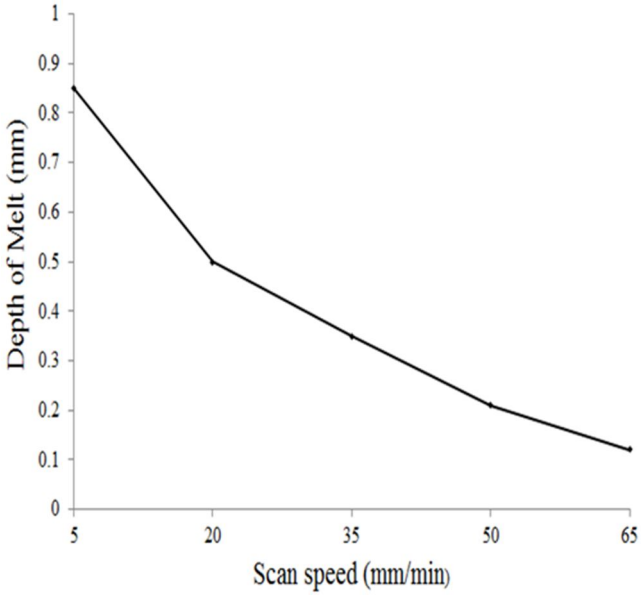

Fig. 9. Influence of laser scan speed on depth of melt (Laser power, 60 W)

The change of melt depth is attributed to the heat conducted to the polymer per unit time at a point as the laser moves across the joint path. At the lowest scan speeds, the polymer is melted to the highest depth due to higher temperatures resulting from long residence time of the laser beam. The converse is true for higher scan speeds.

3.3 Temperature Distribution across the Joint Width

Figure 10 shows the temperature distribution across the width of the polymer for the laser power of 60 W and 70 W. In this figure, the width is along the y-axis as shown in Fig. 2. It can be seen that the temperatures are maximum at the origin, and they drop away from the region. The analysis is done for half the width, since the material is symmetrical. From the graph, it is seen that the lower limit for melting temperature of the polymer (475 K) corresponds to about 2.2 mm and 2.5 mm for the laser power of 60 W and 70 W, respectively. Thus, the full widths of melt at this temperature are 4.4 mm i.e. (2.2× 2) and 5 mm (2.5× 2), respectively. The predicted widths of melt for other conditions are similarly deduced.

The predicted and measured widths of melt for different levels of laser power are compared in Figure 11. The values for the measured widths are obtained

from experimental results by Tillman et al. [23]. The comparison is carried out for the same parameters as those reported in Tillman's experimental work.

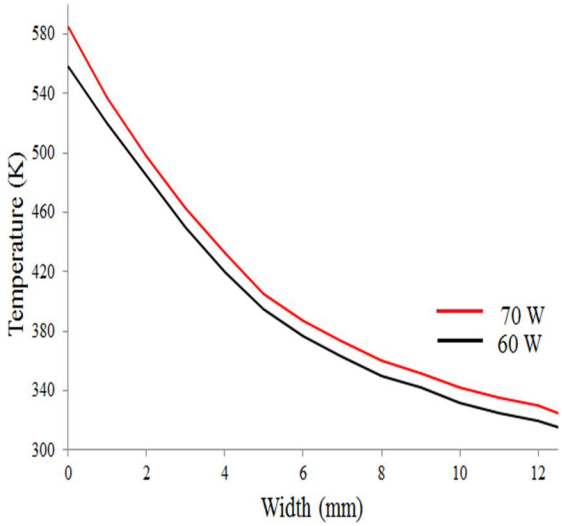

Fig. 10. Temperature distribution across the width for different laser power

It can be seen in Fig 11 that the predicted width of melt closely compares with the measured bond width in experiments. The melt width increases with increase in laser power. This increase is because of higher laser intensity at the interface as the laser power is increased. The theoretical model overestimates the bond width by up to 0.3mm, which represents a deviation of 6%. The difference between the predicted and measured values could be attributed to the simplifying assumptions made for the model. For instance, the effect of mass flow of the melt front for the polymer and nature of the effect of surface topography, which is known to affect the conductance, were not considered in the model.

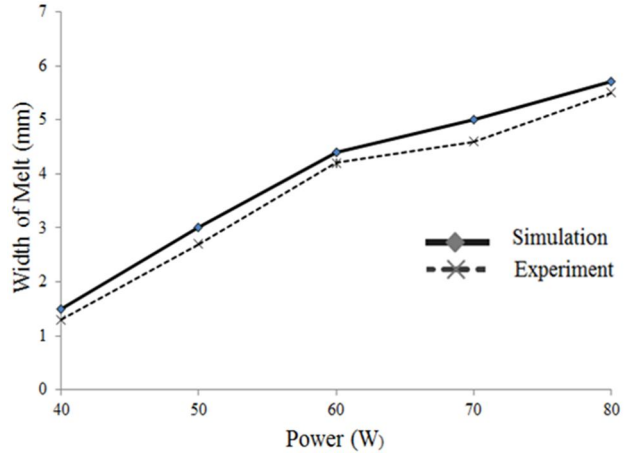

Fig. 11. Influence of different laser power on width of melt (Scan speed, 30 mm/min)

Figure 12 shows the temperature distribution across the width of the polymer for the laser scan speeds of 20 mm/min and 35 mm/min. It is seen that just as was the case for different laser powers (Fig. 10), the temperatures are maximum at the origin, and they drop as one move away from the origin. Similarly, it can be deduced that half the widths of the melt are 2.3 mm and 1.8 mm, which results to 4.6mm and 3.6 mm actual widths, for the scan speeds of 20 mm/min and 35 mm/min, respectively.

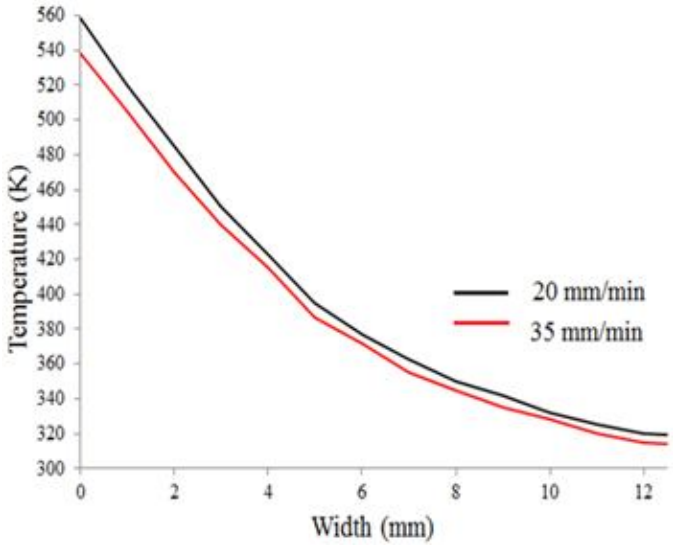

Fig. 12. Temperature distribution across the width for different scan speeds

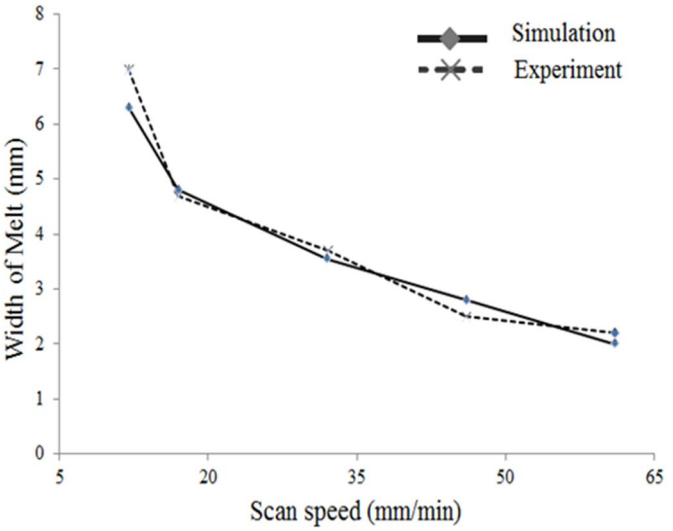

Fig. 13. Influence of different scan speeds on depth of melt (Laser power, 60 W)

The predicted and measured widths of melt for different laser scan speeds are compared in Figure 13. The values for the measured widths are obtained from experimental

results by Tillman et al. [23]. It is seen in the figure, the width of melt decreases with increase in scan speed. The speed has a bearing on the residence time of laser at a spot which in turn has an effect on absorption of heat into the material. Further, it is seen that the predicted and experimental results show a good agreement.

4. Conclusions

A model for predicting the joint temperature, width and depth of melt during laser assisted metal-polymer joining has been developed. The model, which utilizes the material properties and heat transfer characteristics, is tested for joining of SUS304 with Polyethylene Terephthalate material.

From the analysis, it has been seen that laser the parameters have a significant influence on the interface temperatures. The increase of laser power leads to an increase of interface temperatures while increasing the scan speed leads to decreasing temperatures. Consequently, they influence the bond width of the joint. Increasing interface temperatures leads to increasing bond width and depth of the joint. However, while choosing the dimension, proper melting should be ensured to avoid inadequate or excessive heating for proper melting of the polymer.

Optimal temperatures for joining with a laser power of 60 W are achieved at scan speeds ranging between 20-35 mm/min. A comparison made between the predicted melt widths with published experimental results showed good agreement.

References

[1] P. Kah, R. Suoranta, J. Martikainen, and C. Magnus, “Techniques for joining dissimilar materials: Metals and polymers,” Rev. Adv. Mater. Sci., vol. 36, no. 2, pp. 152–164, 2014.

[2] T. Markovits and A. Bauernhuber, “Analysing the thermal characteristics of LAMP joining,” Prod. Eng., vol. 3, no. 2, pp. 14–17, 2014.

[3] Y. Kawahito, A. Tange, S. Kubota, and S. Katayama, “Development of Direct Laser Joining for Metal and Plastic,” in ICALEO, 2006, pp. 376–382.

[4] S. Katayama, Y. Kawahito, Y. Niwa, and S. Kubota, “Laser assisted Metal and Plastic Joining,” in 5th Laser Assisted Net Shape Engineering, 2007, pp. 41–51.

[5] S. Katayama and Y. Kawahito, “Laser direct joining of metal and plastic,” Scr. Mater., vol. 59, no. 12, pp. 1247–1250, 2008.

[6] S. Katayama and Y. Kawahito, “Evolution of LAMP Joining to Dissimilar Materials,” Trans. JWRI, vol. 39, no. 2, pp. 268–269, 2010.

[7] L. Georgiev, T. Sultana, R. J. Baird, G. Auner, G. Newaz, R. Patwa, and H. H., “Laser bonding and characterization of Kapton® FN/Ti and Teflon® FEP/Ti systems,” J Mater. Sci., vol. 44, no. 8, pp. 882–888, 2009.

[8] X. Wang, P. Li, Z. Xu, X. Song, and H. Liu, “Laser transmission joint between PET and titanium for biomedical application,” J Mater. Proc. Tech., vol. 210, no. 13, pp. 1767–1771, 2010.

[9] J. Holtkamp, A. Roesner, and A. Gillner, “Advances in hybrid laser joining,” Int J Adv Manuf Tech, vol. 47, no. 6, pp. 923–930, 2010.

[10] A. Roesner, S. Scheik, A. Olowinsky, A. Gillner, U. Reisgen, and M. Schleser, “Laser assisted joining of plastic metal hybrids,” Phys. Procedia, vol. 12, no. PART 2, pp. 373–380, 2011.

[11] A. Fortunato, G. Cuccolini, A. Ascari, L. Orazi, G. Campana, and G. Tani, “Hybrid metal-plastic joining by means of laser,” Int. J. Mater. Form., vol. 3, no. SUPPL. 1, pp. 1131–1134, 2010.

[12] F. Yusof, M. Yukio, M. Yoshiharu, M. Hamdi, and A. Shukor, “Effect of anodizing on pulsed Nd : YAG laser joining of polyethylene terephthalate (PET) and aluminium alloy (A5052),” J. Mater., vol. 37, pp. 410–415, 2012.

[13] J. Kwang-woon, K. Yousuke, and K. Seiji, “Laser Direct Joining of CFRP to Metal or Engineering Plastic †,” vol. 42, no. 2, pp. 5–8, 2013.

[14] A. Heckert and M. F. Zaeh, “Laser surface pre-treatment of aluminium for hybrid joints with glass fibre reinforced thermoplastics,” Phys. Procedia, vol. 56, no. C, pp. 1171–1181, 2014.

[15] P. Amend, C. Mohr, and S. Roth, “Experimental investigations of thermal joining of polyamide aluminum hybrids using a combination of mono- and polychromatic radiation,” Phys. Procedia, vol. 56, no. C, pp. 824–834, 2014.

[16] A. Cenigaonaindia, F. Liebana, A. Lamikiz, and Z. Echegoyen, “Novel Strategies for Laser Joining of Polyamide and AISI 304,” Phys. Procedia, vol. 39, pp. 92–99, 2012.

[17] A. Roesner, A. Olowinsky, and A. Gillner, “Long term stability of laser joined plastic metal parts,” Phys. Procedia, vol. 41, pp. 169–171, 2013.

[18] K. Van Der Straeten, I. Burkhardt, A. Olowinsky, and A. Gillner, “Laser-induced self-organizing microstructures on steel for joining with polymers,” Phys. Procedia, vol. 83, pp. 1137–1144, 2016.

[19] P. Amend, T. Häfner, M. Gränitz, S. Roth, and M. Schmidt, “Effect of Ultrashort Pulse Laser Structuring of Stainless Steel on Laser-based Heat Conduction Joining of Polyamide Steel Hybrids,” Phys. Procedia, vol. 83, pp. 1130–1136, 2016.

[20] A. Heckert, C. Singer, M. F. Zaeh, R. Daub, and T. Zeilinger, “Gas-tight Thermally Joined Metal-thermoplastic Connections by Pulsed Laser Surface Pre-treatment,” Phys. Procedia, vol. 83, pp. 1083–1093, 2016.

[21] K. Schricker, M. Stambke, J. P. Bergmann, and K. Bräutigam, “Laser-Based Joining of Thermoplastics to Metals : Influence of Varied Ambient Conditions on Joint Performance and Microstructure,” vol. 2016, 2016.

[22] S. P. Dwivedi, S. Sharma, and V. Singh, “Optimization of laser transmission joining process parameters on joint width of PET and 316L stainless steel joint using RSM,” J. Opt., vol. 45, no. 2, pp. 106–113, 2016.

[23] W. Tillmann, A. Elrefaey, and L. Wojarski, “Toward process optimization in laser welding of metal to polymer Prozessoptimierung beim Laserstrahlschweißen von Metall mit Kunststoff,” no. 10, pp. 879–883, 2010.

[24] B. Acherjee, a Kuar, S. Mitra, and D. Mitra, “Finite element simulation of laser transmission welding of dissimilar materials between polyvinylidene fluoride and titanium,” Int. J. Eng. Sci. Technol., vol. 2, no. 4, pp. 176–186, 2010.

[25] E. Rodriguez-Vidal, J. Lambarri, C. Soriano, C. Sanz, and G. Verhaeghe, “A combined experimental and numerical approach

to the laser joining of hybrid polymer - Metal parts," Phys. Procedia, vol. 56, no. C, pp. 835–844, 2014.
[26] Mark Alger, Polymer Science Dictionary. 1997.
[27] P. Ghosh and P. P. Haltu, "Polymer Science-Thermal transitions in polymers," 2006.
[28] BASF, "Laser Welding of Engineering Plastics." pp. 1–8, 2013.
[29] H. K. Webb, J. Arnott, R. J. Crawford, and E. P. Ivanova, "Plastic degradation and its environmental implications with special reference to poly(ethylene terephthalate)," Polymers (Basel)., vol. 5, no. 1, pp. 1–18, 2013.
[30] H. F. Brinson and B. Catherine, Polymer Engineering Science and and Viscoelasticity. Springer Science, 2008.
[31] S. Al-AbdulRazzak and S. . Jabarin, "Processing characteristics of poly(ethylene terephthalate): hydrolytic and thermal degradation," Polym. Int, pp. 167–173, 2002.
[32] C. L. Beyler and M. Hirschler, Thermal Decomposition of polymers.